Applications of a Bayesian biomass dynamic model to Indian Ocean Skipjack (*Katsuwonus pelamis*)

Prepared for the Indian Ocean Tuna Commission

September 30, 2020

Report prepared by:
Charles T T Edwards

For any information regarding this report please
contact the author at:

CESCAPE Consultancy Services
32 Waihoanga Road
Otaki 5582
New Zealand

Email: cescapecs@gmail.com
Telephone: +64-21-575879

CESCAPE Client Report

Client project code:	MTF/INT/661/MUL (TFAA970097099)
Project name:	Fisheries Management Strategy Evaluation
Project end date:	May 31, 2021
Date of report:	September 30, 2020
Prepared for:	IOTC Working Party on Methods, October 2020

Contents

Project Background and Objectives

Based on simulation evaluations of candidate harvest control rules by Adam and Bentley (2013), Bentley and Adam (2014a,b, 2015, 2016), reviewed and endorsed by the Working Party on Tropical Tunas (WPTT), Working Party on Methods (WPM), and the Scientific Committee (SC), the IOTC adopted Resolution 16/02 "On Harvest Control Rules for Skipjack in the IOTC Area of Competence." This described the harvest control rule (HCR) to be used for setting a recommended catch for skipjack (SKJ) and stated that its first implementation will be based upon the 2017 stock assessment agreed by the WPTT and then endorsed by SC. Implementation of the HCR to give a recommended catch limit for 2018–2020 is described in IOTC (2017a). The Resolution also requested a further review and possible modification of the HCR to be conducted no later than 2021.

In 2018, the IOTC WPM noted that the SKJ HCR is not a fully specified Management Procedure (MP), since the underlying data required and assessment methodology are not part of Resolution 16/02. Hence the WPM suggested that the review and potential revision required under Resolution 16/02 be conducted with the aim of determining a full MP for SKJ. This was noted by the SC in 2018.

An MP includes the assessment or estimation method on which the HCR is based, as well as the data inputs and the HCR itself. To be fully specified therefore, a suitable assessment method is required: one that is capable of forming the basis for implementation of the HCR but simple enough to simulation test. A biomass dynamic model could fulfill these requirements. Developing such a model provides the motivation and basis for the current work.

1 Introduction

Biomass dynamic models in fisheries have a long history of application. Because fisheries data are generally collected over discrete timesteps, the models themselves are also usually written in discrete form, with a production function $g(x_t)$, that combines the contributions of recruitment, growth and natural mortality to the dynamics. Written in terms of the current depletion x_t relative to the biomass at unexploited equilibrium K:

$$x_{t+1} = x_t + g(x_t) - H_t \tag{1}$$

where $H_t = C_t/K$ is the harvest rate. This type of model was first applied within a fisheries context by Schaefer (1954, 1957), who implemented a logistic production function:

$$g(x_t) = r \cdot x_t \cdot (1 - x_t) \tag{2}$$

This has two estimable parameters, usually referred to as the intrinsic rate of population growth r and the carrying capacity K.

The logistic model has a number of useful reference points associated with it that can be obtained directly from parameter estimates. These correspond to a maximum sustainable yield $\text{MSY} = r \cdot K/4$ and the associated harvest rate $H_{\text{MSY}} = r/2$. If we define the ratio $\phi = x_{\text{MSY}}$, then the logistic model specifically assumes that $\phi = 0.5$ (i.e. MSY is achieved at half the carrying capacity). However this is usually inconsistent with predictions made by age-structured fisheries models, which are based on a stock-recruitment function that often predicts $\phi < 0.5$. It is therefore desirable to implement a biomass dynamic model that has reference points consistent with an age-structured analogue.

The logistic model was generalized by Pella and Tomlinson (1969) to allow $\phi \neq 0.5$ by introducing a shape parameter p:

$$g(x_t) = (r/p) \cdot x_t \cdot \left(1 - x_t^p\right) \tag{3}$$

This was subsequently re-paramaterised by Fletcher (1978) in terms of a shape parameter n and $m = \text{MSY}$. However, depending on ϕ, both formulations of this generalized production function are capable of predicting excessively high per capita growth at low biomass levels. For $p \leq 0$, corresponding to $\phi \leq e^{-1} \approx 0.37$, the intrinsic growth rate becomes infinite. This is a strong caveat against use of this model for fisheries in which we might assume that $0.2 < \phi < 0.4$.

For the generalized production function, there is no single parameter that predicts population growth at low biomass levels. For the logistic model, in contrast, the intrinsic growth is defined by the parameter r as the maximum rate of increase as the biomass (or depletion) converges on zero:

$$r = \lim_{x \to 0} \frac{1}{x} \frac{\mathrm{d}\, x}{\mathrm{d}\, t} \tag{4}$$

This is useful because it allows a prior to be constructed for r using life-history theory (McAllister et al., 2001) or meta-analysis.

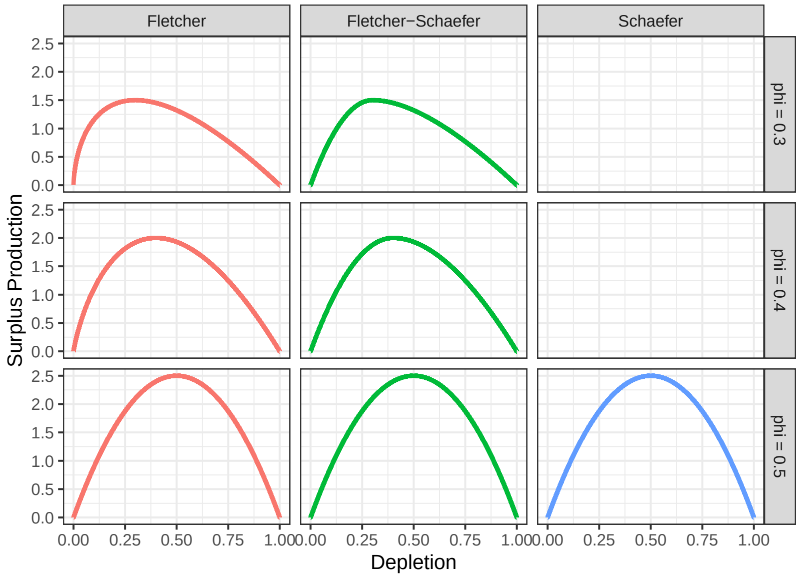

Figure 1: Production functions for different models assuming $r = 0.1$ and $\phi = 0.3, 0.4, 0.5$

1.1 The hybrid model

It is preferable in fisheries modelling to use a model that allows for $\phi < 0.5$ and has an ecologically consistent parameter for the maximum intrinsic growth rate. One solution to this problem was proposed by McAllister et al. (2000) in the form of a combined Fletcher-Schaefer hybrid model. It has a discontinuous inflection point at x_{MSY} with dynamics for values of $x < x_{\text{MSY}}$ governed by the logistic (Schaefer) model, and dynamics at higher biomass levels governed by the generalized (Fletcher) production model. The model can be written as:

$$g(x_t) = \begin{cases} r \cdot x_t \cdot \left(1 - \dfrac{x_t}{2 \cdot \phi}\right) & \text{if } x \leq \phi \\ \gamma \cdot m \cdot (x_t - {x_t}^n) & \text{if } x > \phi \end{cases} \tag{5}$$

$$\phi = \left(\frac{1}{n}\right)^{(1/(n-1))} \tag{6a}$$

$$\gamma = \frac{n^{\,n/(n-1)}}{n-1} \tag{6b}$$

$$m = \frac{r \cdot \phi}{2} \tag{6c}$$

Reference points are: $\text{MSY} = m \cdot K$, $x_{\text{MSY}} = \phi$ and $H_{\text{MSY}} = r/2$.

It is informative to compare these generalised and hybrid models at different ϕ values. Figures 1 and 2 show the production functions and per capita growth for $0 \leq x \leq 1$, assuming $r = 0.1$ and $\phi = \{0.3, 0.4, 0.5\}$. The Fletcher model notably exaggerates the productivity at low biomass levels. This problem is resolved by the Fletcher-Schaefer hybrid. The Fletcher-Schaefer hybrid model is therefore preferred here, and implemented in the **bdm** package.

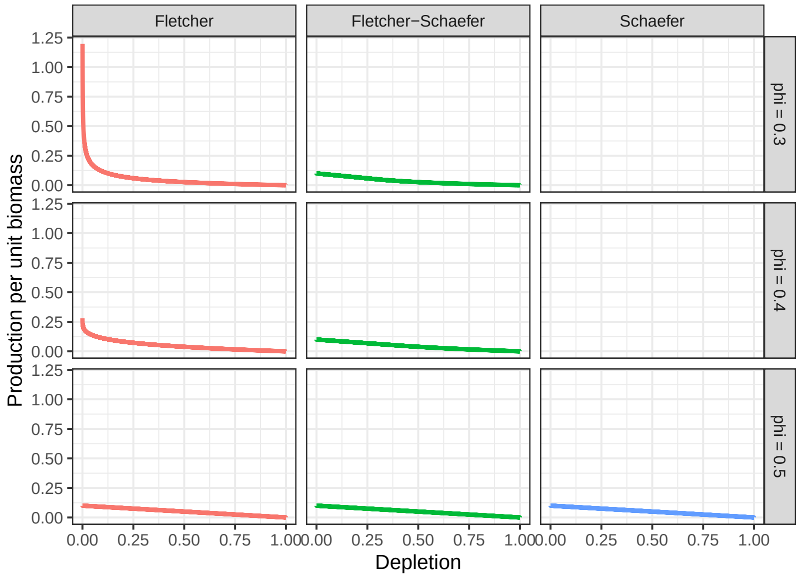

Figure 2: Growth rate per capita as a function of biomass assuming $r = 0.1$ and $\phi = 0.3, 0.4, 0.5$

1.2 The bdm package

The **bdm** package fits a state-space biomass dynamic model using Bayesian methods, specifically the Hamiltonian MCMC implemented in the package **rstan** (R Core Team, 2020, Stan Development Team, 2020). An advantage of this class of models is that they allow both process and observation error to be represented simultaneously, which is important for effective precautionary or risk based management (Harwood and Stokes, 2003). To a large extent, **bdm** is an external wrapper for **rstan**, providing functionality relevant to the intended application. The package is generalisable, meaning that any number of model formulations can be specified by the user. The default implements the Fletcher-Schaefer hybrid model (Equation 5), with $\phi = 0.5$ (i.e. $n = 2$) specified as an input value, making it equivalent to the logistic model.

The model formulates the process equation to include a time-dependent error term (the process error, ϵ^p) and a parallel observation process that relates an abundance index y_{it} to the unobserved depletion state with some degree of error (the observation error, ϵ^o), according to a catchability scalar q_i:

$$x_{t+1} = [x_t + g(x_t) - H_t] \cdot \epsilon^p_t \tag{7a}$$

$$y_{it} = [q_i \cdot x_t] \cdot \epsilon^o_{it} \tag{7b}$$

where i refers to a particular abundance index. The process and observation equations assume log-Normal error distributions:

$$x_t \sim LN\left(\log(\bar{x}_t) - \sigma_p^2/2, \sigma_p^2\right) \tag{8}$$

$$y_{it} \sim LN\left(\log(\bar{y}_t) - \sigma_o^2/2, \sigma_o^2\right) \tag{9}$$

where $\bar{x}_t$ and $\bar{y}_t$ are the deterministic predictions, formulated such that:

$$\mathbb{E}[x_t] = \bar{x}_t \tag{10a}$$

$$\mathbb{E}\left[y_{it}\right] = \bar{y}_t \tag{10b}$$

and with an initial condition of $\bar{x}_{t=0} = 1$. Parameters to be estimated in the model are r, K and the process error scale term σ_p. This requires integration across both the process and observation error residuals, and q_i for each index, which is treated as a nuisance parameter. The observation error scale terms σ_o are fixed on input. The shape parameter ϕ is poorly estimated by this class of model (Clark et al., 2010) and was therefore also fixed on input.

Prior distributions for the estimated parameters are:

$$r \sim LN(\mu_r, \sigma_r^2) \tag{11a}$$

$$\log(K) \sim Uniform(a, b) \tag{11b}$$

$$\sigma_p \sim Exponential(\lambda) \tag{11c}$$

Including an exponential prior on σ_p places a double exponential constraint on $\log(x)_t$ (Andrews and Mallows, 1974), and therefore implements a form of adaptive shrinkage (Park and Casella, 2008). We used a fixed input value of $\lambda = 10$, which gives $\mathbb{E}\left[\sigma_p\right] = 0.1$. The uniform prior on $\log(K)$ adds a penalty to the posterior proportional to $1/K$, making it useful for preventing excessively large values. Bounds of $a = 1$ and $b = 12$ were chosen based on preliminary fits to the data. Finally an informative distribution on r is helpful due to the fact that r and K are highly correlated within the model, and is often necessary for convergence. A log-Normal distribution is recommended by McAllister et al. (2001), since it provides a good description of priors for r constructed using Monte-Carlo sampling of life-history data.

The catchability q is estimated analytically from its maximum posterior density estimate assuming an uninformative uniform prior (i.e. $q \sim U(.,.)$).

$$\hat{q}_i = \exp\left[\frac{1}{n_t}\sum_t \left\{\log(y_{it}) - \log(x_t)\right\} + \frac{\sigma_o^2}{2}\right] \tag{12}$$

If we assume that the biomass is exactly known for purposes of the estimation of $\hat{q}$, then $\mathbb{E}\left[\log(x_t)\right] = \log(x_t)$. Since $\mathbb{E}\left[\log(y_{it})\right] = \log(q_i \cdot x_t) - \sigma_o^2/2$, then $\mathbb{E}\left[\log(\hat{q}_i)\right] = \mathbb{E}\left[\log(q_i)\right]$ and $\mathbb{E}\left[\hat{q}_i\right] = \mathbb{E}\left[q_i\right]$ as required:

$$\begin{aligned}
\mathbb{E}\left[\log(\hat{q}_i)\right] &= \left[\frac{1}{n_t}\sum \left\{\mathbb{E}\left[\log(y_{it})\right] - \mathbb{E}\left[\log(x_t)\right]\right\} + \frac{\sigma_o^2}{2}\right] \\
&= \left[\frac{1}{n_t}\sum \left\{\log(q_i \cdot x_t) - \frac{\sigma_o^2}{2} - \log(x_t)\right\} + \frac{\sigma_o^2}{2}\right] \\
&= \log(q_i)
\end{aligned} \tag{13}$$

2 Indian Ocean Skipjack

2.1 Empirical Data

Catch and abundance data for the years 1950 to 2016, per quarter, were obtained directly from the 2017 skipjack stock assessment (IOTC, 2017c). Three catch rate indices were available and are plotted in Figure 3, with the catches shown in Figure 4. Catches were assumed to be known, whereas abundance was assumed observed with a standard error of $\sigma_o = 0.2$ for all indices.

2.2 Prior for the intrinsic growth

Attempts to obtain an informative prior using life-history theory were unsuccessful (yielding anomalously large values, $r > 1$). We therefore obtained a prior from `fishbase.org`, which reports $r = 0.57$ with a 95% confidence interval of $(0.37-0.85)$. Given that $\mathbb{E}[r] = \exp(\mu_r + \sigma_r^2/2)$, assuming a log-Normal distribution this equates to values of $\mu_r \approx -0.58$ and $\sigma_r \approx 0.2$. We used the **lhm** package to construct a prior on this basis (Figure 5). Noting that it is a quarterly model, this gives prior input values of $\mu_r = -1.97$ and $\sigma_r = 0.2$ (Equation 11a). However throughout this report, unless otherwise indicated, we refer to r as an annual value.

2.3 Model explorations

An initial ("Reference") model fit was performed with $\phi = 0.4$, consistent with the assumption of $B_{MSY}/B_0 = 0.4$ used in in the stock assessment (IOTC, 2017c), and $\mathbb{E}[r] = 0.6$. Three MCMC chains were run for 10000 iterations each, keeping every third sample. They converged reasonably well (Figure 6) with strong updates to $\log(K)$ and σ_p (Figures 7 and 8). Fits are shown in Figure 9. Estimated reference points and status metrics are listed in Table 1. A kobe phase plot is given in Figure 10.

The Reference model outputs are consistent with the stock being close to MSY. This is in accord with outputs from the grid of Stock Synthesis III assessment model runs, which used $SSB_{40\%}$ as a proxy for the biomass at MSY, and which reports median values of $SSB_{2016}/SSB_0 = 0.4$, an exploitation rate relative to the exploitable biomass of $E_{2016}/E_{40\%} = 0.93$ and MSY $= 510.1$ thousand tonnes (IOTC, 2017b). The Reference model presented here estimates MSY $= 438.04$ thousand tonnes.

Table 1: Reference model outputs from fit of biomass dynamic model to quarterly data on catch and abundance, assuming $\mathbb{E}[r] = 0.6$ and $\phi = 0.4$. Biomass values (written as $x_t \cdot K$) are given in units of 1000 tonnes.

Metric	Median and 90% CI
$^*r$	0.13 (0.09–0.18)
$\log(K)$	8.35 (8.01–8.91)
*MSY	109.51 (90.31–171.22)
x_{MSY}	0.4 (0.4–0.4)
$x_{MSY} \cdot K$	1692.12 (1209.43–2969.67)
$x_{2016} \cdot K$	1761.84 (1095.96–3907.01)
x_{2016}	0.42 (0.33–0.56)
x_{2016}/x_{MSY}	1.05 (0.82–1.41)
$^*H_{MSY}$	0.07 (0.05–0.09)
$^*H_{2016}$	0.07 (0.03–0.11)
$^*H_{2016}/H_{MSY}$	1.07 (0.53–1.57)

*given as quarterly values

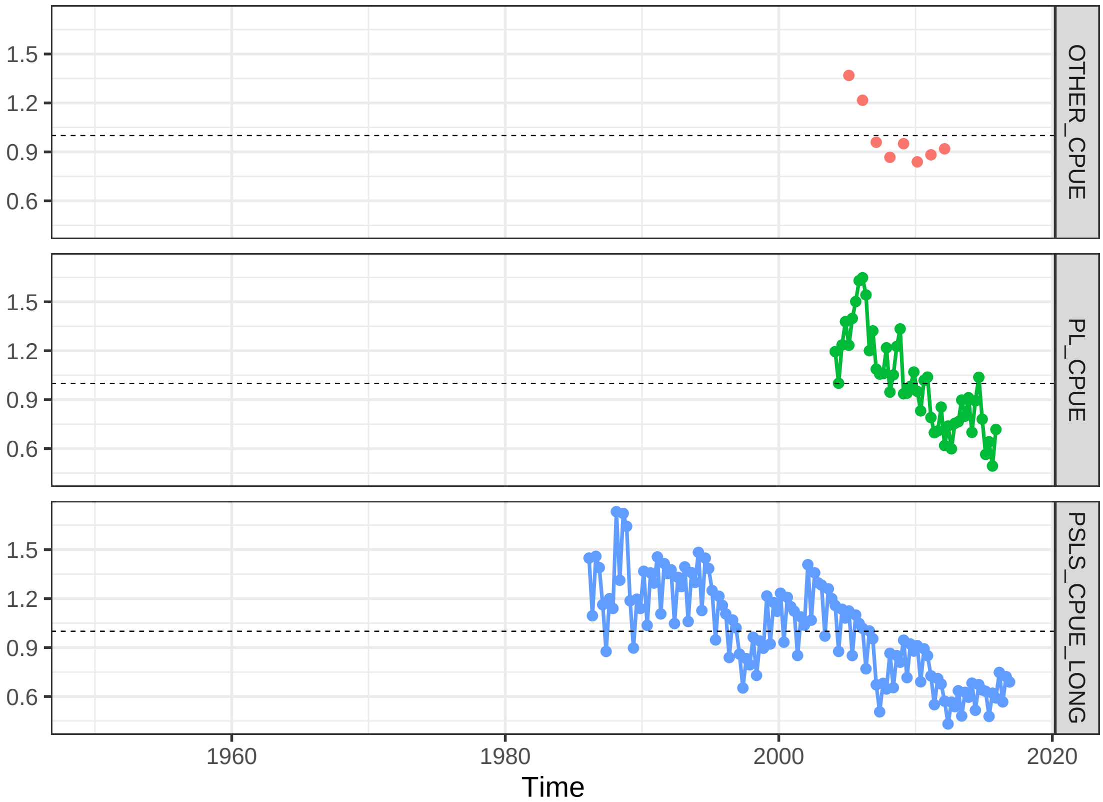

Figure 3: Catch rate indices per quarter, renormalised to an arithmetic mean of one.

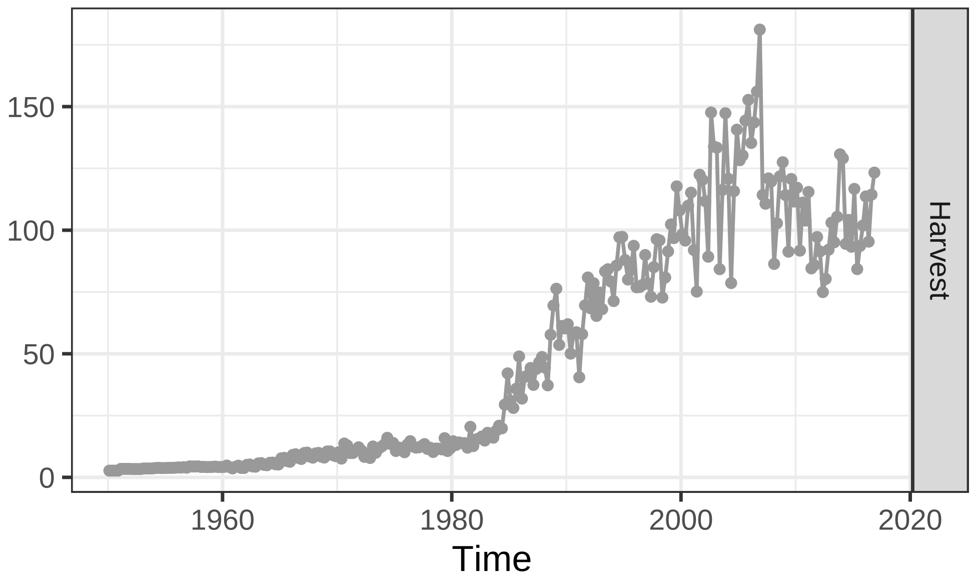

Figure 4: Catch (thousand tonnes) per quarter.

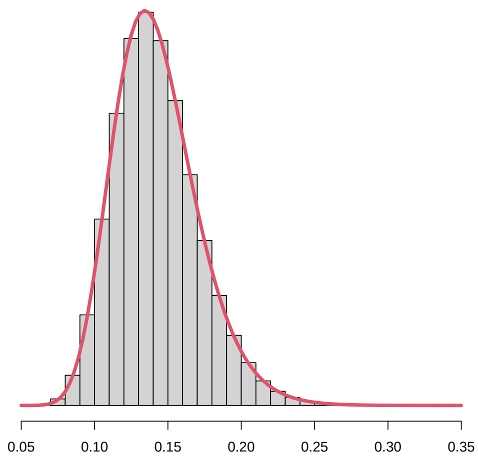

Figure 5: Prior for the intrinsic growth

Alternative models were used to examine sensitivity of the outputs to different assumptions regarding ϕ and $\mathbb{E}[r]$, specifically all combinations of $\phi = \{0.3, 0.4, 0.5\}$ and $\mathbb{E}[r] = \{0.5, 0.6, 0.7\}$. Prior updates are shown in Figure 11. Estimated dynamics are shown in Figures 12, 13 and 14.

We can consider sensitivity of the model predictions using either absolute values or values relative to the MSY reference point. Considering depletion, the model predicts a similar level of depletion in the current year irrespective of the $\mathbb{E}[r]$ and ϕ input values assumed (Figure 12). However the x_{MSY} reference point is a function of ϕ (by definition), and therefore stock status relative to x_{MSY} is dependent on this input assumption. Smaller values of ϕ imply a more optimistic depletion status. Concerning the biomass, large values of K are typically associated with low values of r and vice versa (Figure 11). Higher input values for $\mathbb{E}[r]$ will therefore lead to smaller estimates of K and lowever overall biomass (Figure 13). However status relative to the reference point $x_{\text{MSY}} \cdot K$ will be unchanged, since K cancels out. This can be seen in Table 2, since values of $x_{2016} \cdot K$ and x_{2016} relative to their MSY reference points are identical.

Harvest rates over time (by quarter) are shown in Figure 14. The harvest rate at MSY is $H_{\text{MSY}} = r/2$ and is therefore dependent on the input assumption concerning $\mathbb{E}[r]$, but independent of ϕ. The estimate of K will also be sensitive to $\mathbb{E}[r]$, and since $H_t = C_t/K$, larger values of $\mathbb{E}[r]$, leading to smaller values of K, predict a higher harvest rate. Both H_{2016} and H_{MSY} therefore share a positive correlation with $\mathbb{E}[r]$. We can see this from Table 2: assuming $\phi = 0.4$ the estimated quarterly harvest rate increases from $H_{2016} = 0.06$ when $\mathbb{E}[r] = 0.5$ to $H_{2016} = 0.08$ when $\mathbb{E}[r] = 0.7$; equivalent to annual rates of $20 - 30\%$. However for the same value of ϕ status relative to the H_{MSY} reference point is essentially unchanged. There is a caveat however, in that surplus production is also dependent on ϕ (Figure 1), with smaller values of ϕ predicting lower productivity at equivalent depletion levels. At smaller ϕ the model therefore requires a lower harvest rate to generate the same depletion dynamics. This has a more noticeable effect on the estimated harvest rate compared to the assumptions regarding $\mathbb{E}[r]$. In summary therefore, we can conclude that relative estimates of the harvest rate are robust to input assumptions concerning $\mathbb{E}[r]$ but not ϕ.

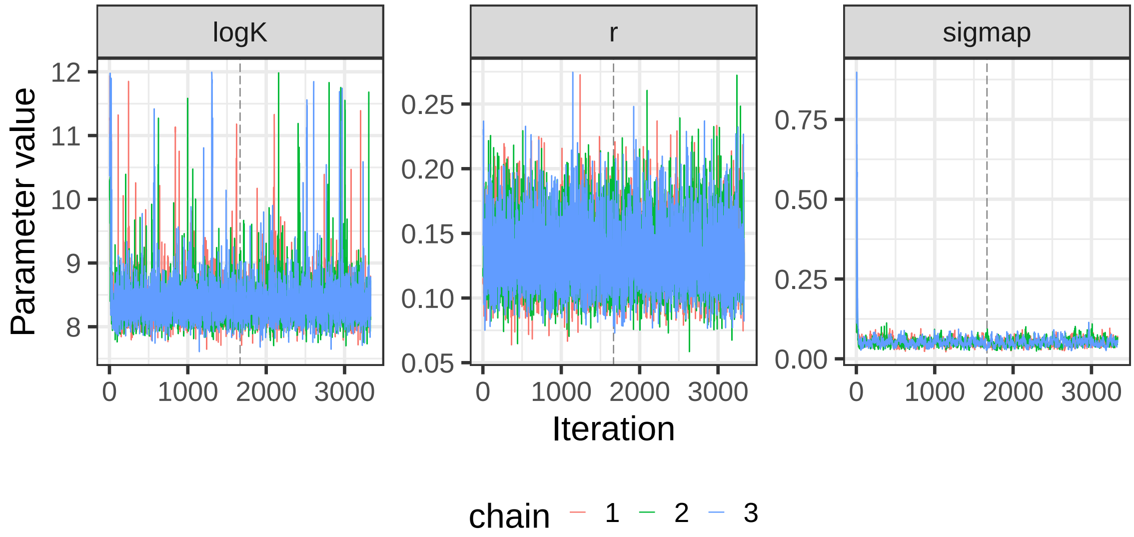

Figure 6: Trace plots following reference model fit.

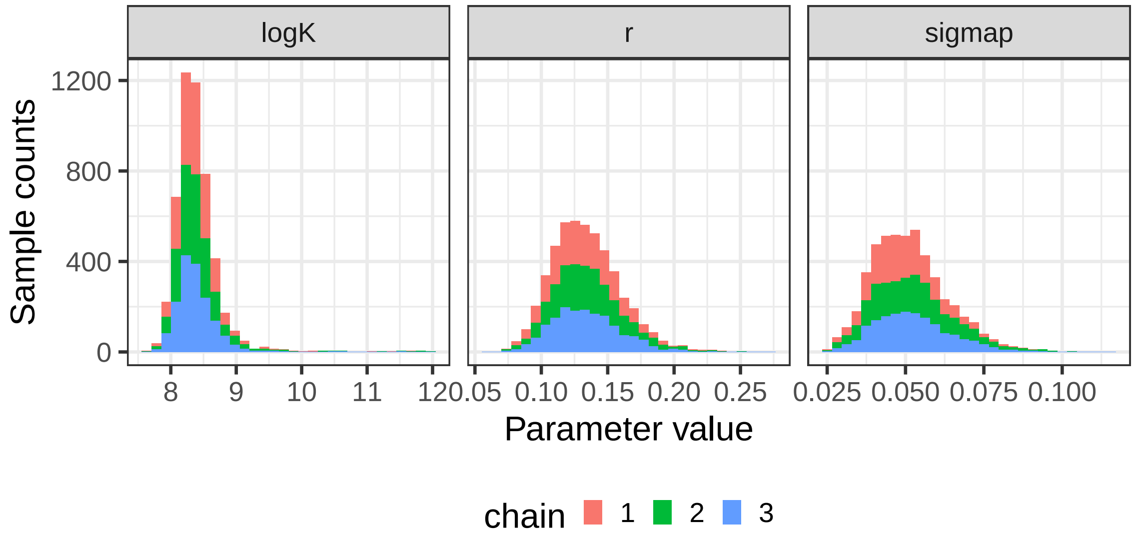

Figure 7: Posterior histogram plots following reference model fit

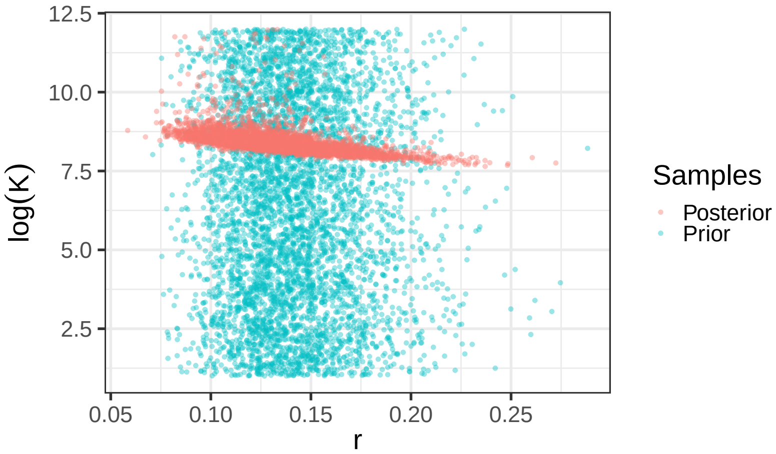

Figure 8: Prior updates following reference model fit, showing individual samples from the prior and posterior distributions.

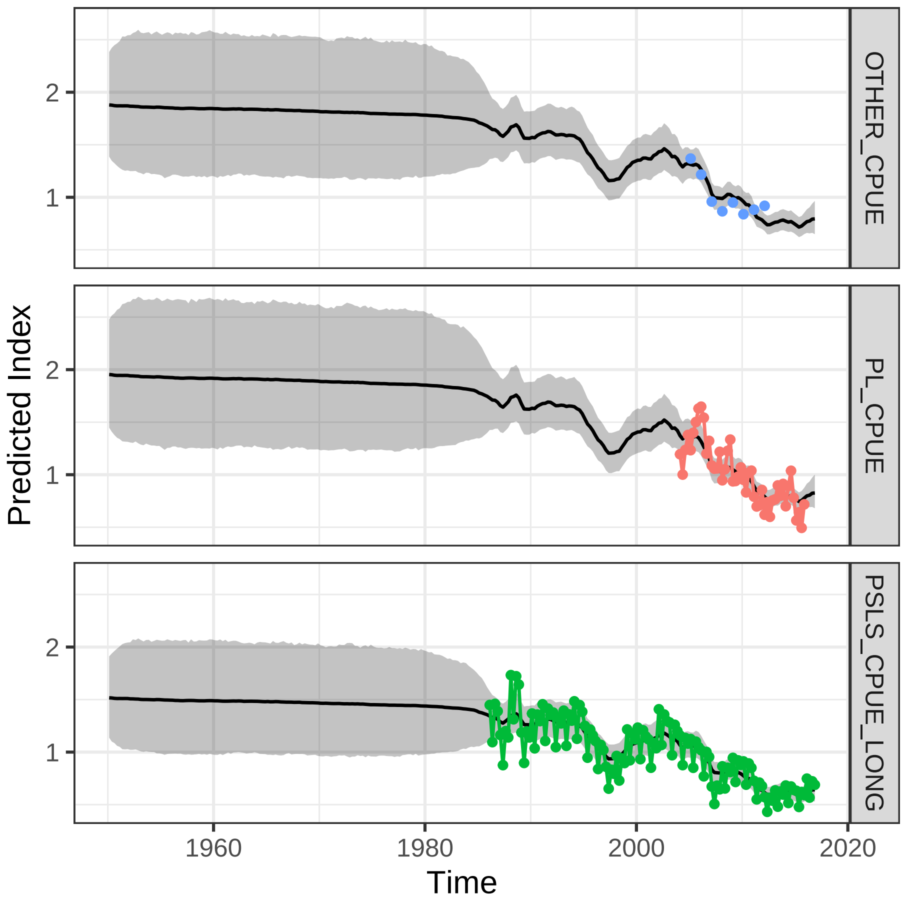

Figure 9: Fits to CPUE series. Median and 90% credibility intervals are shown.

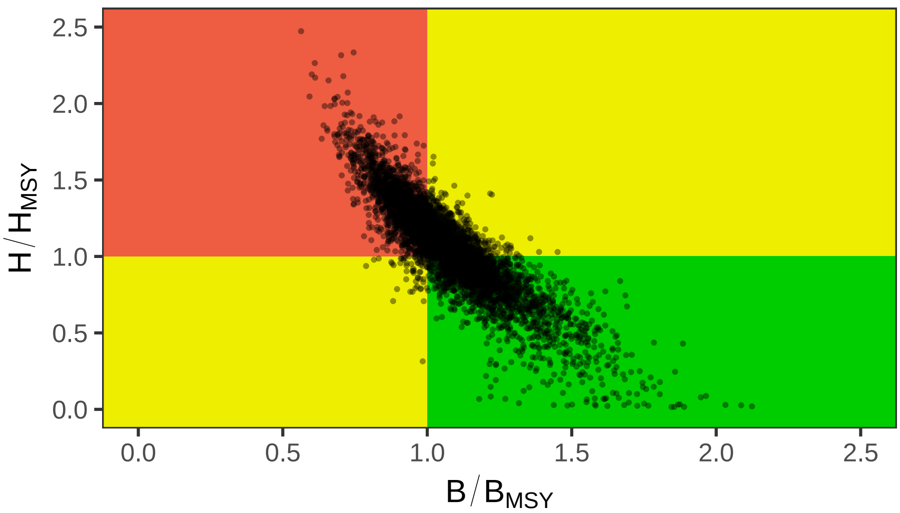

Figure 10: Kobe phase plot showing posterior distribution of current (2016) stock status relative to reference points assuming $\phi = 0.4$ and $\mathbb{E}[r] = 0.6$

Table 2: Model estimates for the current biomass (in thousand tonnes), current depletion (relative to K) and current harvest rate given alternative inputs values of $\mathbb{E}[r]$ and ϕ. Median and 90% CI are given. Relative values are proportional to the associated MSY reference point.

Metric	$\mathbb{E}[r]$	ϕ	Value	Relative value
$x_{2016} \cdot K$	0.5	0.3	2857.28 (1566.2–18691.69)	1.45 (1.04–2.20)
	0.5	0.4	1948.49 (1218.48–4642.39)	1.05 (0.81–1.43)
	0.5	0.5	1539.39 (1014.49–2721.84)	0.84 (0.68–1.07)
	0.6	0.3	2349.79 (1345.57–9045.42)	1.42 (1.04–2.08)
	0.6	0.4	1659.41 (1042.71–3739.22)	1.05 (0.81–1.42)
	0.6	0.5	1329.90 (887.5–2321.81)	0.85 (0.68–1.08)
	0.7	0.3	2058.54 (1196.01–5867.56)	1.41 (1.05–1.97)
	0.7	0.4	1472.42 (924.27–2905.46)	1.05 (0.81–1.37)
	0.7	0.5	1158.34 (786.03–1886.62)	0.85 (0.68–1.06)
x_{2016}	0.5	0.3	0.43 (0.31–0.66)	1.45 (1.04–2.20)
	0.5	0.4	0.42 (0.33–0.57)	1.05 (0.81–1.43)
	0.5	0.5	0.42 (0.34–0.54)	0.84 (0.68–1.07)
	0.6	0.3	0.43 (0.31–0.62)	1.42 (1.04–2.08)
	0.6	0.4	0.42 (0.32–0.57)	1.05 (0.81–1.42)
	0.6	0.5	0.43 (0.34–0.54)	0.85 (0.68–1.08)
	0.7	0.3	0.42 (0.31–0.59)	1.41 (1.05–1.97)
	0.7	0.4	0.42 (0.32–0.55)	1.05 (0.81–1.37)
	0.7	0.5	0.42 (0.34–0.53)	0.85 (0.68–1.06)
$^*H_{2016}$	0.5	0.3	0.04 (0.01–0.08)	0.73 (0.12–1.25)
	0.5	0.4	0.06 (0.03–0.10)	1.08 (0.49–1.61)
	0.5	0.5	0.08 (0.05–0.12)	1.38 (0.87–1.87)
	0.6	0.3	0.05 (0.01–0.09)	0.75 (0.21–1.21)
	0.6	0.4	0.07 (0.03–0.12)	1.08 (0.53–1.58)
	0.6	0.5	0.09 (0.05–0.14)	1.35 (0.88–1.82)
	0.7	0.3	0.06 (0.02–0.10)	0.74 (0.29–1.18)
	0.7	0.4	0.08 (0.04–0.13)	1.06 (0.60–1.53)
	0.7	0.5	0.11 (0.07–0.16)	1.34 (0.92–1.78)

*quarterly values

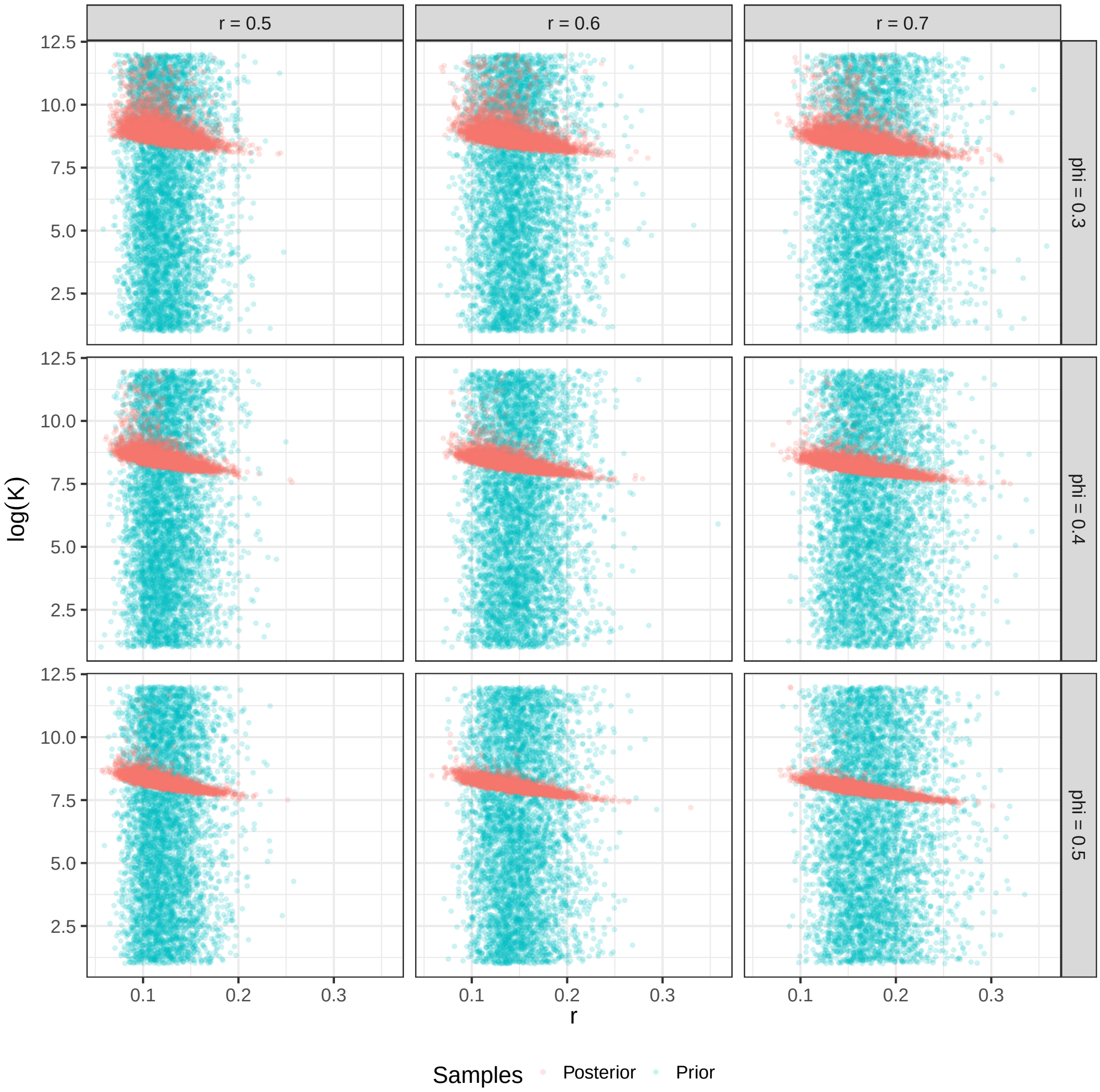

Figure 11: Prior updates for alternative input values of $\mathbb{E}[r]$ and ϕ, showing individual samples from the prior and posterior distributions.

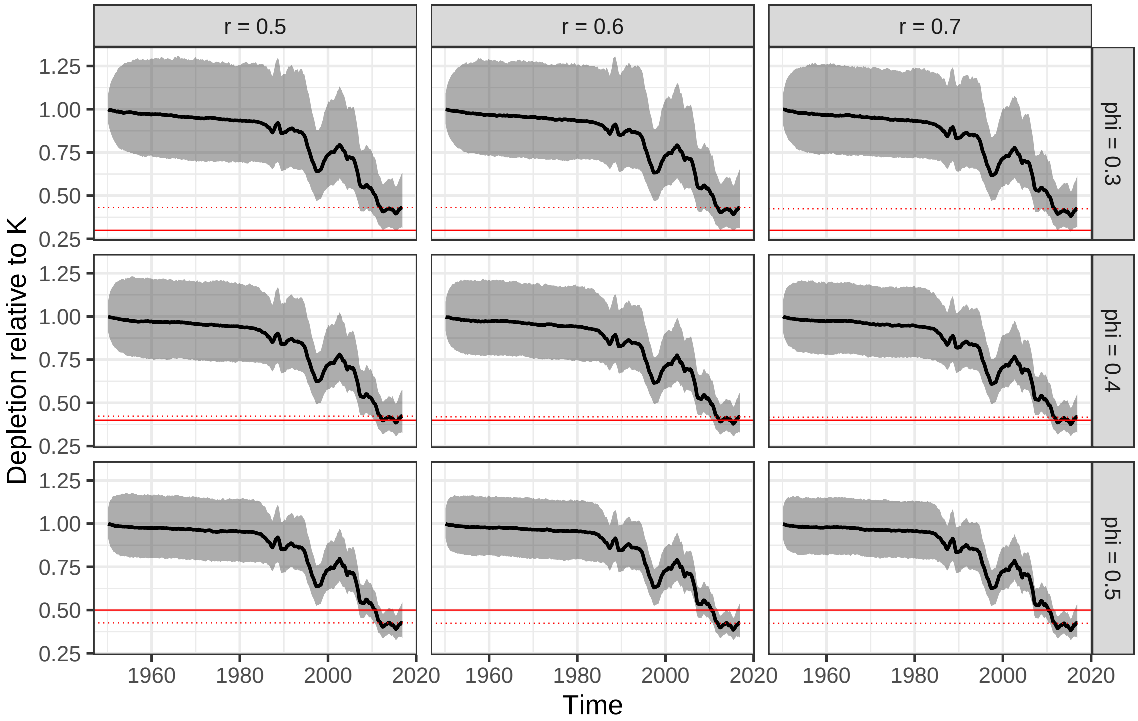

Figure 12: Comparative depletion dynamics for alternative input values of $\mathbb{E}[r]$ and ϕ. Median and 90% credibility intervals are shown, with the current depletion (dashed red line) and depletion-based reference point x_{MSY} (solid red line) also shown.

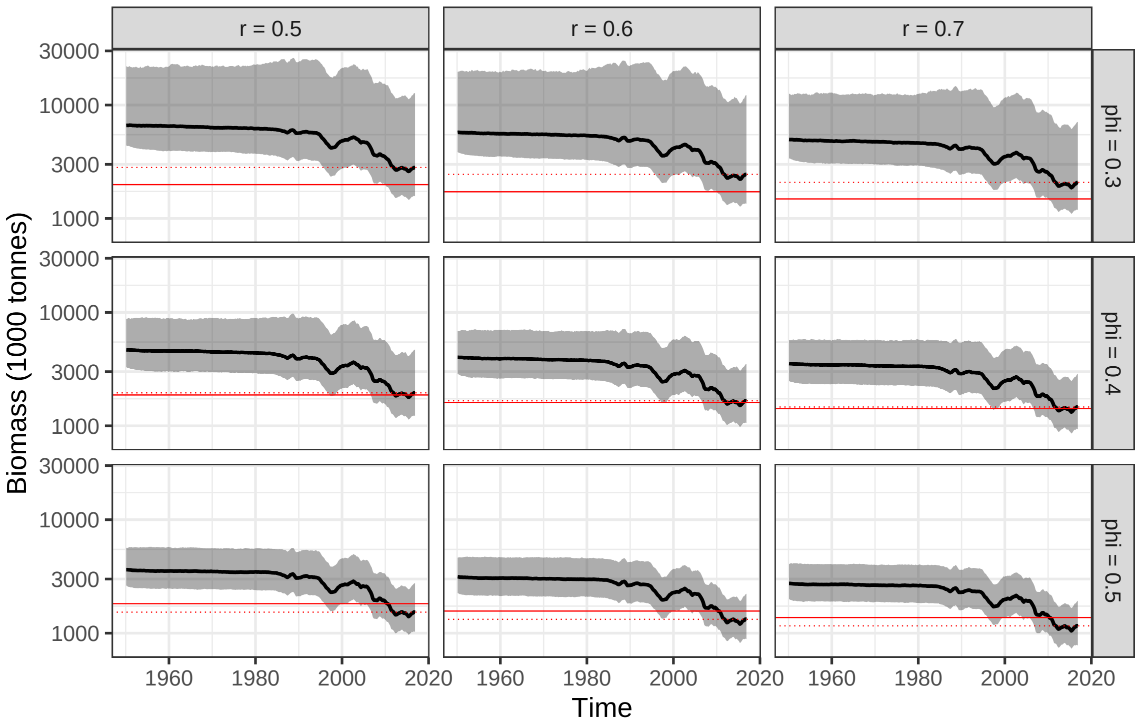

Figure 13: Comparative biomass dynamics for alternative input values of $\mathbb{E}[r]$ and ϕ, with biomass given in units of 1000 tonnes and plotted on a log10-scale. Median and 90% credibility intervals are shown, with the current biomass (dashed red line) and biomass at MSY reference point $K \cdot x_{MSY}$ (solid red line) also shown.

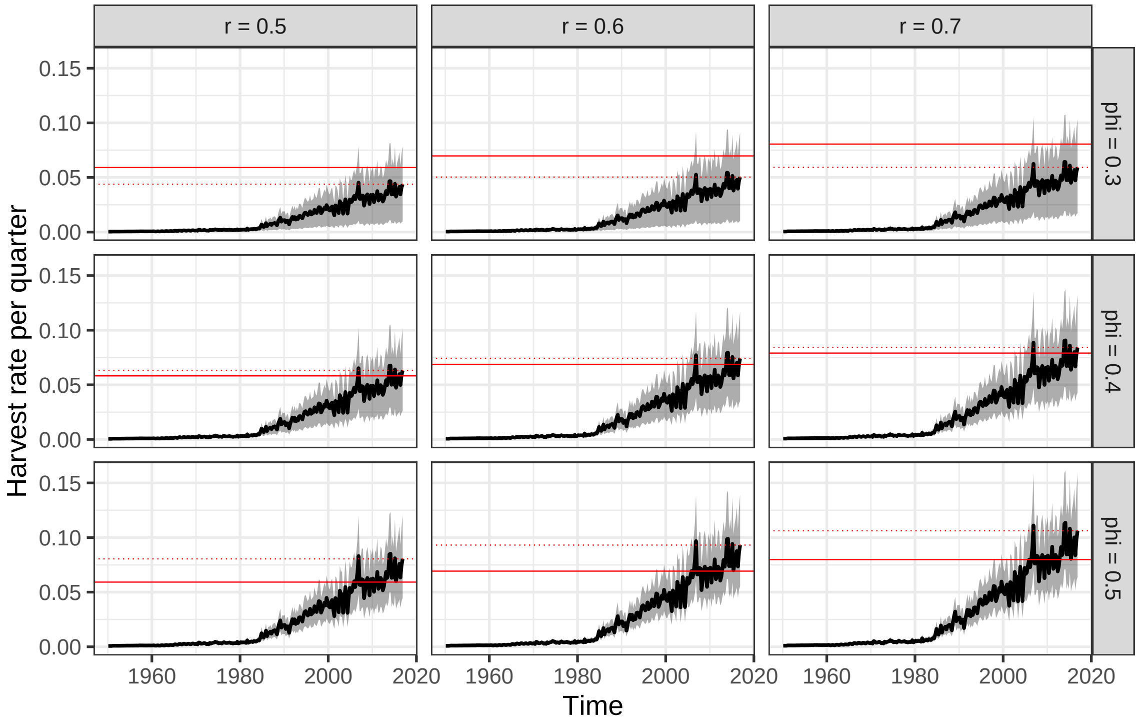

Figure 14: Comparative harvest rate dynamics for alternative input values of $\mathbb{E}[r]$ and ϕ, with harvest rate given as a proportion of the biomass caught per quarter. Median and 90% credibility intervals are shown, with the current harvest rate (dashed red line) and harvest rate at MSY reference point $H_{\text{MSY}} = r/2$ (solid red line) also shown.

3 Summary and Conclusions

From fits of the Reference model it is possible to generate stock status estimates, relative to MSY reference points (Figure 10), that are similar to those produced by the Stock Synthesis III stock assessment (IOTC, 2017c). However explorations of alternative input parameters show that these status estimates are sensitive to model assumptions. In particular, both the depletion status x_t/x_{MSY} and harvest rate H_t/H_{MSY} are noticeably dependent on the input value of ϕ (Table 2). Fortunately however, they appear insensitive to input prior values of $\mathbb{E}[r]$, which is a useful result. Finally we are able to conclude that x_t, the depletion relative to K, is robust to the complete range of input assumptions explored (Figure 15), whereas the havest rate H_t, is robust to input values concerning $\mathbb{E}[r]$ but not ϕ (Figure 16). Estimation of the stock status is therefore feasible, but dependent on choosing an appropriate assumption concerning shape of the production function.

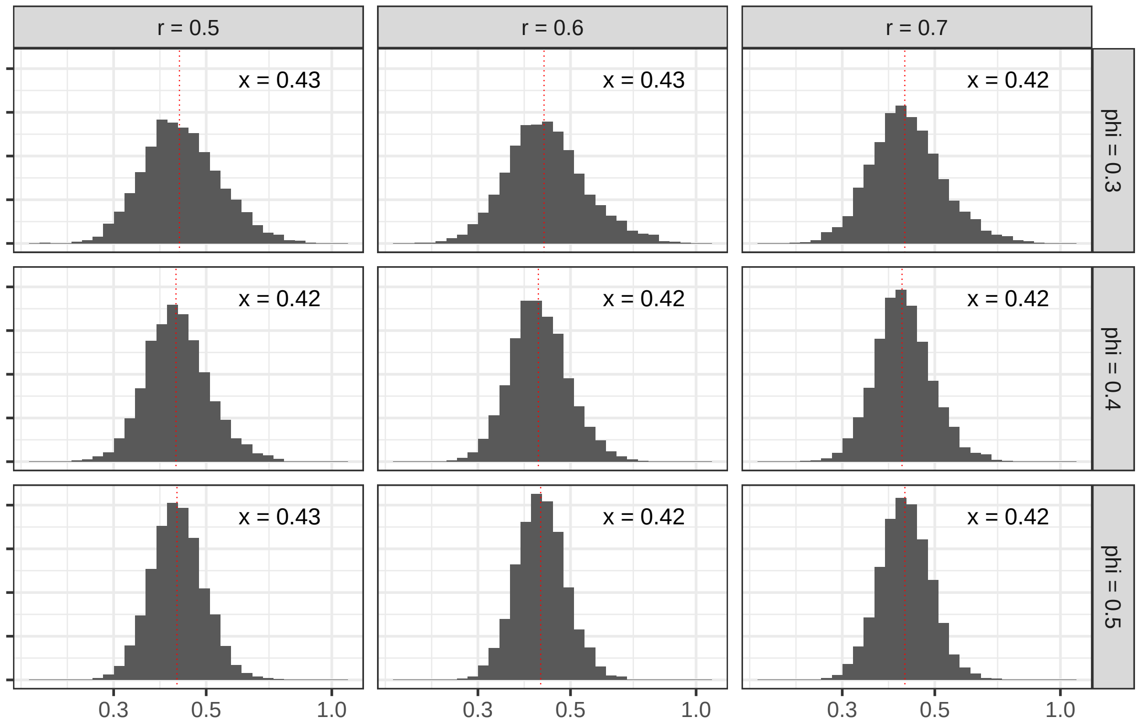

Figure 15: Comparative posterior estimates of the current depletion x_{2016}. The full posterior distribution is shown with the median value also given.

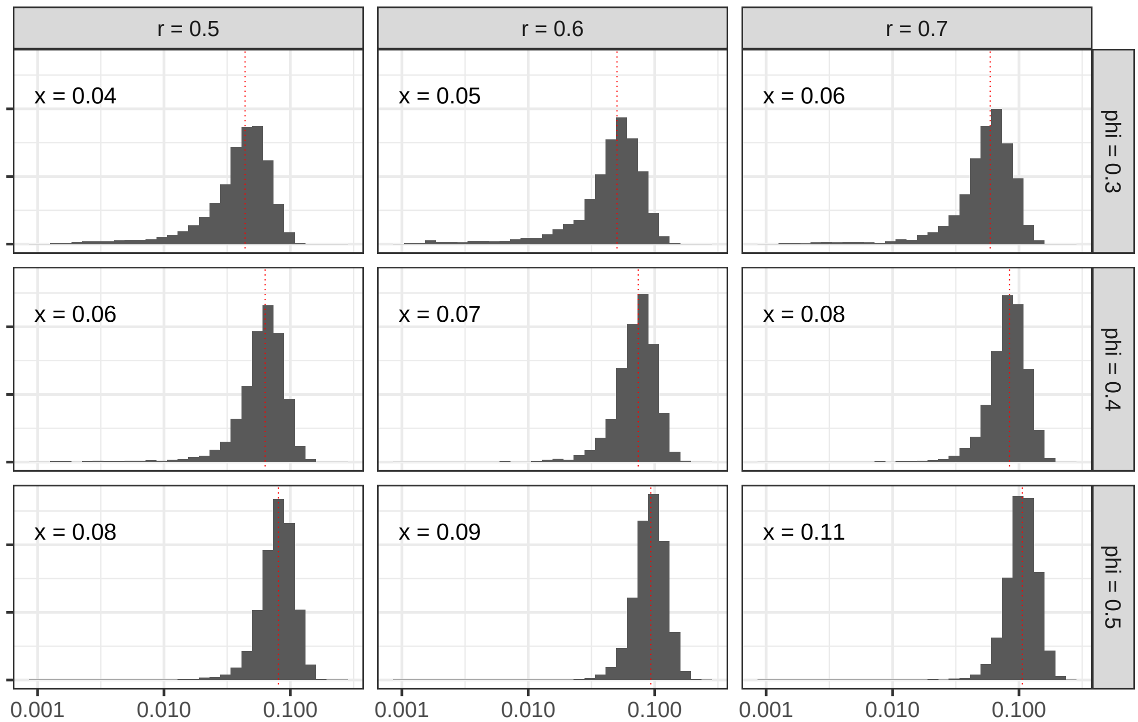

Figure 16: Comparative posterior estimates of the current harvest rate H_{2016}. The full posterior distribution is shown with the median value also given.

4 Model code

Reference code implemented for the current project is stored in `https://github.com/cttedwards/bdm` and `https://github.com/cttedwards/lhm`.

5 Acknowledgments

This work was funded by the Indian Ocean Tuna Commission, under project code MTF/INT/661/MUL. Initial development of the **bdm** and **lhm** R-packages was funded by NIWA (Wellington, New Zealand) under project codes FIFI1402, FIAR1503, with support from M. K. McAllister (University of British Columbia, Canada).

6 References

Adam, S., Bentley, N., 2013. Progress and arrangements for Management Strategy Evaluation work of Indian Ocean Skipjack Tuna. Final Research Report (IOTC-2013-WPTT15-42) .

Andrews, D.F., Mallows, C.L., 1974. Scale mixtures of normal distributions. Journal of the Royal Statistical Society: Series B (Methodological) 36, 99–102.

Bentley, N., Adam, S., 2014a. Management procedure evaluation for the Indian Ocean skipjack tuna fishery: model description and conditioning. Final Research Report (IOTC-2014-WPM05-08) .

Bentley, N., Adam, S., 2014b. Management Strategy Evaluation for Indian ocean skipjack tuna: first steps. Final Research Report (IOTC-2014-WPTT16-39) .

Bentley, N., Adam, S., 2015. An operating model for the Indian Ocean skipjack tuna fishery. Final Research Report (IOTC-2015-WPTT17-35) .

Bentley, N., Adam, S., 2016. Management strategy evaluation for the Indian Ocean skipjack tuna Fishery. Final Research Report (IOTC-2016-WPM07-15 Rev 1) .

Clark, F., Brook, B.W., Delean, S., Reşit Akçakaya, H., Bradshaw, C.J.A., 2010. The theta-logistic is unreliable for modelling most census data. Methods in Ecology and Evolution 1, 253–262.

Fletcher, R.I., 1978. On the restructuring of the pella-tomlinson system. Fishery Bulletin 76, 515–521.

Harwood, J., Stokes, K., 2003. Coping with uncertainty in ecological advice: lessons from fisheries. Trends in Ecology & Evolution 18, 617 – 622.

IOTC, 2017a. Calculation of Skipjack catch limit for the period 2018-2020 using the harvest control rule adopted in Resolution 16/02. IOTC–2017–SC20-12 Rev 1 .

IOTC, 2017b. Calculation of Skipjack catch limit for the period 2018-2020 using the harvest control rule adopted in Resolution 16/02. IOTC–2017–SC20-12 Rev 1 .

IOTC, 2017c. Indian ocean skipjack tuna stock assessment 1950-2016 (stock synthesis). IOTC OTC–2017–WPTT19–47 rev1.

McAllister, M.K., Babcock, E.A., Pikitch, E.K., Prager, M.H., 2000. Application of a non-equilibrium generalized production model to south and north atlantic swordfish: combining bayesian and demographic methods for parameter estimation. Collected Volume of Scientific Papers ICCAT 51, 1253–1550.

McAllister, M.K., Pikitch, E.K., Babcock, E.A., 2001. Using demographic methods to construct bayesian priors for the intrinsic rate of increase in the schaefer model and implications for stock rebuilding. Canadian Journal of Fisheries and Aquatic Sciences 58, 1871–1890.

Park, T., Casella, G., 2008. The bayesian lasso. Journal of the American Statistical Association 103, 681–686.

Pella, J.J., Tomlinson, P.K., 1969. A generalized stock production model. Inter-American Tropical Tuna Commission Bulletin 13, 421–496.

R Core Team, 2020. R: A Language and Environment for Statistical Computing. URL: https://www.R-project.org/. version 4.0.2.

Schaefer, M.B., 1954. Some aspects of the dynamics of populations important to the management of commercial marine fisheries. Bulletin of the Inter-American Tropical Tuna Commission Bulletin 1, 26–56.

Schaefer, M.B., 1957. A study of the dynamics of the fishery for yellowfin tuna in the eastern tropical pacific ocean. Bulletin of the Inter-American Tropical Tuna Commission Bulletin 2, 247–285.

Stan Development Team, 2020. RStan: the R interface to Stan. URL: http://mc-stan.org/. R package version 2.21.2.